ACTIVE FLUTTER SUPPRESSION*

A. Bradshaw, T. Rahulan and M. A. Woodhead
Department of Aeronautical and Mechanical Engineering
University of Salford, Salford M5 4WT, U.K.

Abstract

A new theory is presented in this paper which makes use of acceleration components along with other parameters in the design of control systems. This theory is illustrated by designing an integrated digital flight control system to suppress flutter in a wind tunnel model. The understanding of the flutter mechanism, led to an approach that was based on forced frequency separation and this method is shown to be very efficient in delaying the onset of flutter. The implementational problems were then examined and a technique is presented which enables the control architecture to be simplified. Digital simulations of transient responses are presented for two different sensor configurations when the model is subjected to a discrete gust.

1. Introduction

The application of active control technology to flutter suppression in aircraft is comparatively new. Flutter is an explosive phenomenon in which the aircraft structure absorbs excess energy from the aerodynamic forces through interacting natural modes. If uncontrolled, flutter instability can rapidly destroy the aircraft structure. Passive control of flutter usually results in expensive structural modifications along with weight penalties and reduced speed capabilities. Active methods incorporating feedback principles may be used by exploiting existing control surfaces to improve the dynamic performance with negligible weight penalties. The artificial stability thus provided also has the effect of reducing structural and fatigue loads and results in greater ride comfort due to the attenuation of aircraft rigid body and flexural motions.

There has been a clear division between the theoretical and the implementational aspects of active flutter suppression. Theoretical work, although mathematically rigorous, has tended to be rather too refined for implementation in real systems. Little consideration has been given by the theoreticians to the practical implementation of their theoretical designs. Almost invariably, the implications of the dynamical characteristics of the actuators and the sensors are ignored; control algorithms which require the use of state observers are proposed; and it has been tacitly assumed that reliable digital implementation of complex control algorithms are available. All these features imply additional phase lags which significantly affect the performance of the control system. On the other hand, most of the successful wind tunnel and flight test demonstrations have employed techniques based more on experience and intuition rather than purely theoretical concepts. As a result, simpler basic control strategies have been derived, the implementation of which has been achieved by the use of standard equipment such as compensators, phase adjusters and notch filters. It is also quite common to feed back the rate of change of the states in practice whereas theoretical analyses have concentrated almost entirely on state feedback. This has arisen chiefly because rate feedback automatically introduces phase lead which compensates for the phase lag of various items of equipment in the feedback loop and hence gives satisfactory transient responses. In this paper, a new theory is presented in which some of the state variable rates, the accelerations, are fed back for control purposes.

This paper is concerned with the theoretical and computational work that was carried out to derive an integrated digital flight control system with the following features:

a) use of rate feedback for flutter suppression and load alleviation with disturbance rejection qualities only;

b) use of state feedback for rigid body motion control with disturbance rejection and set point tracking capabilities;

and

c) the use of the minimum number of sensors such that the actual outputs approximate to the theoretically prescribed values.

The controller design techniques are illustrated by considering the active control of the GARTEUR wind tunnel model[1] in an open-loop unstable flight mode configuration. This linearised model of the longitudinal dynamics includes the first three symmetric elastic modes in addition to the basic pitch and heave modes of motion. The active inputs are the angular deflections of the taileron, the outer wing flaperon, and the inner wing flaperon. Feedback information is used to vary the control surface deflections so that the model is stabilised and the structural loads reduced in magnitude. The improvements in performance are demonstrated by the presentation of the results of a digital computer study in which the controlled model is subjected to a simulated discrete gust.

In the studies carried out earlier[2] (using state feedback only), the following points were noted.

a) In the open-loop stable configurations (i.e. at lower speeds), the GARTEUR model presented little problems and the controller could be configured such that the system was always stable for any overall gain; the motion attenuation performance being dictated by control equipment capabilities.

b) In the open-loop unstable configuration, it was clear that for system stability, the

*Sponsored by MOD Research Agreement 2101/063 (XR/ST)

minimum control surface deflections required were rather large (up to 15^{o} deflection for the inner wing flaperon). This situation would degrade even further when control equipment dynamics are introduced in the feedback loops.

Hence, for this paper, it was decided to disregard the open-loop stable configurations and concentrate only on the open-loop unstable configuration with digital control.

One of the classic features of the flutter phenomenon is that the instability is associated with the frequency coalescence of two modes (they can be either structural and/or rigid body modes). Hence the approach adopted was based on the separation of the coalescing modes rather than the 'traditional' feedback of the unstable modes. This approach is not very successful with state feedback control but, when the rates of change of the states are considered for feedback, the results obtained are excellent. These results show that there is no need to include all the inputs in the control structure and consequently one of the control surfaces (the inner flaperon) can be deleted from the original system.

There is also a need to use as few sensors as possible in order to ease implementation for wind tunnel testing. This problem can be solved by a study of the effects of contamination of the theoretical measurement requirements with unwanted states and/or their rates. The solution is then arrived at after an iterative series of analyses in which the sensors are successively reconfigured. The use of fewer sensors than the theoretically ideal number results in a degradation of the controlled system performance in some ways. However, the use of the design technique described in this paper minimises this degradation and the implementation problem is greatly eased. Care has been taken to ensure that all the control surface deflections and rates are within the specified limits.

2. Theory

The first part of this section is concerned with the theory for regulation schemes which employ acceleration feedback. An asymptotic analysis is developed which reveals the underlying dynamical structure of such closed-loop systems. The theory is then extended to allow the incorporation of position and velocity measurements in the active control scheme so that multifunctional control systems can be designed which employ acceleration feedback terms for stabilization and regulation, and position and velocity terms for command tracking.

2.1 System Description

The equations of motion of structures naturally arise in the second-order form[3]

$$M\ddot{q} + L\dot{q} + Kq = Nu + d \qquad (2.1)$$

where $q \in R^{n}$ is the vector of generalised displacements, $u \in R^{\ell}$ is the vector of control input actions, $d \in R^{n}$ is the vector of disturbance inputs, $M \in R^{n \times n}$ is the mass matrix, $L \in R^{n \times n}$ is the damping matrix, $K \in R^{n \times n}$ is the stiffness matrix, and $N \in R^{n \times \ell}$ is the control input matrix. For purposes of analysis it is convenient to recast (2.1) into the form

$$\dot{x} = Ax + Bu + Dd \qquad (2.2)$$

where

$$x = \begin{bmatrix} q \\ \dot{q} \end{bmatrix} \in R^{n}$$

$$A = \begin{bmatrix} 0 & , & I_{n} \\ -M^{-1}K & , & -M^{-1}L \end{bmatrix} \in R^{n \times n}$$

$$B = \begin{bmatrix} 0 \\ M^{-1}\ N \end{bmatrix} \in R^{n \times \ell}$$

$$D = \begin{bmatrix} 0 \\ M^{-1}. \end{bmatrix} \in R^{n \times n}$$

and where $n = 2n$. Note that the state vector, x, contains generalised displacements and velocities and that therefore the state derivative vector, $\dot{x}$, contains velocities and accelerations. For the purpose of feedback control system design it is to be assumed that the disturbance vector, d, cannot be measured.

The object of using feedback control is to improve the tracking response of a system and so also to improve its disturbance rejection qualities. The vector, $y \in R^{\ell}$ can be defined so that it describes the variables being controlled. The elements of y are known as the outputs and can be expressed in terms of the state vector by an equation of the form

$$y = Cx \qquad (2.3)$$

where $C \in R^{\ell x n}$ called the output matrix, contains the necessary relationships between y and x.

Although in certain special cases[4] it is possible to achieve excellent control using output feedback, in general more information is required in order to guarantee stability and to avoid highly oscillatory responses. Additional feedback information can be incorporated and described in terms of the state vector by a feedback equation of the form

$$w = Fx = y + m \qquad (2.4)$$

where $F \in R^{\ell x n}$ is the feedback matrix and $m \in R^{\ell}$ is a vector of extra-measurements such that

$$\lim_{t\to\infty} m = 0 \qquad (2.5)$$

Condition (2.5) can be achieved by using the purely kinematic relations from within the plant. For instance, in some cases,

$$m = \dot{y} \qquad (2.6)$$

and it follows that, in any steady-state condition (2.5) will be satisfied.

When acceleration terms are available for control purposes, the vector $a \in R^{\ell}$ can be defined so that it describes the accelerations in terms of the state derivative vector by an equation of the form

$$a = R\dot{x} \qquad (2.7)$$

where $R \in R^{\ell x n}$ contains the necessary relationships between a and $\dot{x}$. It then follows, using (2.2), that the acceleration vector can be expressed in the form

$$a = RAx + RBu + RDd \qquad (2.8)$$

2.2 Regulation Scheme

In a regulation scheme, proportional feedback of the acceleration vector is used in order to stabilise the system and to improve its disturbance rejection characteristics. If a control-law equation of the form

$$u = gKa \qquad (2.9)$$

is used, where $K \in R^{\ell x \ell}$ and $g \in R^{+}$ then it follows from (2.8) and (2.9) that

$$u = (I_{\ell} - gKRB)^{-1} gKR(Ax + Dd) \qquad (2.10)$$

It then follows from (2.2) and (2.10) that the closed-loop state equation can be expressed in the form

$$\dot{x} = [I_n + B(I_{\ell} - gKRB)^{-1}gKR](Ax + Dd) \qquad (2.11)$$

If a digital control system is to be implemented in which the acceleration vector is sampled at rate f and a piecewise constant control input vector is generated with negligible delay then the discrete-time closed-loop state equation can be expressed in the form

$$x' = [\Phi + \Psi (I_{\ell} - gKRB)^{-1}gKRA]x + [\Xi + \Psi (I_{\ell} - gKRB)^{-1}gKRD]d \qquad (2.12)$$

where

$$\Phi = \exp(AT) \qquad (2.13)$$

$$\Psi = \int_0^T \exp(A(T-\tau))\, B\, d\tau \qquad (2.14)$$

$$\Xi = \int_0^T \exp(A(T-\tau))\, D\, d\tau \qquad (2.15)$$

and

$$T = 1/f \qquad (2.16)$$

2.3 Asymptotic Analysis

The matricial expression $(I_{\ell} - gKRB)^{-1}gKR$ can be expressed in terms of a power series in 1/g as follows

$$(I_{\ell} - gKRB)^{-1}gKR = -(KRB)^{-1}\{I_{\ell} + (KRB)^{-1}/g + (KRB)^{-2}/g^2 + \ldots\}KR. \qquad (2.17)$$

provided that rank $KRB = \ell$. In such cases it follows that

$$\lim_{g\to\infty} (I_{\ell} - gKRB)^{-1}gKR = -(KRB)^{-1}KR = -(RB)^{-1}R \qquad (2.18)$$

The asymptotic form of the control law (2.10) is therefore

$$u = -(RB)^{-1}R(Ax + Dd) \qquad (2.19)$$

and the asymptotic form of the acceleration vector (2.8) then becomes

$$a = 0 \qquad (2.20)$$

Evidently, increasingly effective disturbance rejection characteristics can be expected as $g \to \infty$!

It also follows from (2.11) and (2.18) that the asymptotic form of the closed-loop state equation as $g \to \infty$ is

$$\dot{x} = [I_n - B(RB)^{-1}R](Ax + Dd). \qquad (2.21)$$

Further, by setting g = f it follows that the asymptotic form of the discrete time state equation is

$$x' = \{I_n + T(I_n - B(RB)^{-1}R)A\}x + T(I_n - B(RB)^{-1}R)Dd. \qquad (2.22)$$

Without loss of generality the state equation (2.2) can be expressed in the partitioned form

$$\begin{bmatrix}\dot{x}_1\\ \dot{x}_2\end{bmatrix} = \begin{bmatrix}A_{11} & A_{12}\\ A_{21} & A_{22}\end{bmatrix}\begin{bmatrix}x_1\\ x_2\end{bmatrix} + \begin{bmatrix}0\\ B_2\end{bmatrix}u + \begin{bmatrix}D_1\\ D_2\end{bmatrix}d \qquad (2.23)$$

and the acceleration vector (2.7) can be expressed in the conformable form

$$a = [R_1 \; , \; R_2]\begin{bmatrix}\dot{x}_1\\ \dot{x}_2\end{bmatrix} \qquad (2.24)$$

where $x_1 \in R^{n-\ell}$, $x_2 \in R^{\ell}$ and all the submatrices are dimensioned conformably. If it is assumed that rank $R_2B_2 = \ell$ then the partitioned

form of the closed-loop state equation (2.21) becomes

$$\begin{bmatrix}\dot{x}_1\\ \dot{x}_2\end{bmatrix} = \begin{bmatrix} A_{11} & A_{12} \\ -R_2^{-1}R_1A_{11} & -R_2^{-1}R_1A_{12}\end{bmatrix}\begin{bmatrix}x_1\\ x_2\end{bmatrix} + \begin{bmatrix}D_1\\ -R_2^{-1}R_1D\end{bmatrix}d \tag{2.25}$$

Evidently, as g becomes larger the closed-loop poles approach the sets

$$Z_1 = \{0 : \text{repeated } \ell \text{ times}\} \tag{2.26}$$

and

$$Z_2 = \{\lambda \in C: |\lambda I_{n-\ell} - A_{11} + A_{12} R^{-1}_2 R_1| = 0\} \tag{2.27}$$

Further, the asymptotic form of the closed-loop discrete-time state equation is

$$\begin{bmatrix}x_1'\\ x_2'\end{bmatrix} = \begin{bmatrix} I_{n-\ell} + TA_{11} & TA_{12} \\ -TR_2^{-1}R_1A_{11} & I_\ell - TR_2^{-1}R_1A_{12}\end{bmatrix}\begin{bmatrix}x_1\\ x_2\end{bmatrix} + \begin{bmatrix}TD_1\\ -TR_2^{-1}R_1D_1\end{bmatrix}d \tag{2.28}$$

so that as f becomes large the closed-loop discrete-time poles approach the sets

$$Z_1 = \{1 : \text{repeated } \ell \text{ times}\} \tag{2.29}$$

and

$$Z_2 = \{\lambda\in C: |\lambda I_{n-\ell} - I_{n-\ell} - T(A_{11} - A_{12}R^{-1}_2R_1)| = 0\} \tag{2.30}$$

2.4 Tracking Scheme

The acceleration feedback control of the previous sections can be combined with the regular error-actuated control function. For convenience the open-loop state equation is expressed in the form

$$\begin{bmatrix}\dot{x}_1\\ \dot{x}_2\\ \dot{x}_3\end{bmatrix} = \begin{bmatrix} A_{11} & A_{12} & A_{13}\\ A_{21} & A_{22} & A_{23}\\ A_{31} & A_{32} & A_{33}\end{bmatrix}\begin{bmatrix}x_1\\ x_2\\ x_3\end{bmatrix} + \begin{bmatrix}0\\ B_2\\ 0\end{bmatrix}u_1 + \begin{bmatrix}0\\ 0\\ B_3\end{bmatrix}u_2 + \begin{bmatrix}D_1\\ D_2\\ D_3\end{bmatrix}d \tag{2.31}$$

the acceleration vector is expressed in the form

$$a = [R_1, R_2, 0]\begin{bmatrix}\dot{x}_1\\ \dot{x}_2\\ \dot{x}_3\end{bmatrix} \tag{2.32}$$

and the output vector is expressed in the form

$$y = [C_1, C_2, C_3]\begin{bmatrix}x_1\\ x_2\\ x_3\end{bmatrix} \tag{2.33}$$

where $x_1 \in R^{n-\ell_1-\ell_2}$, $x_2 \in R^{\ell_1}$, $x_3 \in R^{\ell_2}$, $u_1 \in R^{\ell_1}$, $u_2 \in R^{\ell_2}$, $d \in R^q$, $a \in R^{\ell_1}$, $y \in R^{\ell_2}$, and the submatrices are dimensioned conformably. The control law equations can then be expressed in the forms

$$u_1 = gKa \tag{2.34}$$

and

$$u_2 = g[K_0e + K_1z] \tag{2.35}$$

where

$$\dot{z} = e \tag{2.36}$$

and

$$e = v - y \tag{2.37}$$

and where $K \in R^{\ell_1 x \ell_1}$, $K_0 \in R^{\ell_2 x \ell_2}$, $K_1 \in R^{\ell_2 x \ell_2}$, and $g \in R^+$.

The control objectives are to stabilise the closed-loop system, track command inputs v, and reject the unmeasured disturbances d.

It follows from (2.10), (2.31), (2.32) and (2.34) that

$$u_1 = (I_{\ell_1} - gKR_2B_2)^{-1}gK[R_1,R_2,0]\begin{bmatrix} A_{11} & A_{12} & A_{13}\\ A_{21} & A_{22} & A_{23}\\ A_{31} & A_{32} & A_{33}\end{bmatrix}$$

$$\begin{bmatrix} x_1 \\ x_2 \\ x_3 \end{bmatrix} + \begin{bmatrix} D_1 \\ D_2 \\ D_3 \end{bmatrix} d \Bigg] \qquad (2.38)$$

and from (2.33), (2.35) and (2.37) that

$$u_2 = gK_0v - g\,K_0\,[C_1,\ C_2,\ C_3] \begin{bmatrix} x_1 \\ x_2 \\ x_3 \end{bmatrix} + g\,K_1\,z \qquad (2.39)$$

The closed-loop state equation can then be formed from (2.31), (2.38) and (2.39), and expressed in the form

$$\begin{bmatrix} \dot{z} \\ \dot{x}_1 \\ \dot{x}_2 \\ \dot{x}_3 \end{bmatrix} = \Bigg\{ \begin{bmatrix} I_{\ell_2} & 0 & 0 & 0 \\ 0 & I_{n-\ell_1-\ell_2} & 0 & 0 \\ 0 & 0 & I_{\ell_1} & 0 \\ 0 & 0 & 0 & I_{\ell_2} \end{bmatrix} +$$

$$\begin{bmatrix} 0 \\ 0 \\ B_2 \\ 0 \end{bmatrix} (I_{\ell_1} - gKR_2B_2)^{-1} gK\,[0, R_1, R_2, 0] \Bigg\}$$

$$\times \Bigg\{ \begin{bmatrix} 0 & -C_1 & -C_2 & -C_3 \\ 0 & A_{11} & A_{12} & A_{13} \\ 0 & A_{21} & A_{22} & A_{23} \\ 0 & A_{31} & A_{32} & A_{33} \end{bmatrix} \begin{bmatrix} z \\ x_1 \\ x_2 \\ x_3 \end{bmatrix} + \begin{bmatrix} 0 \\ D_1 \\ D_2 \\ D_3 \end{bmatrix} d \Bigg\}$$

$$+ \begin{bmatrix} 0 & , & 0 & , & 0 & , & 0 \\ 0 & , & 0 & , & 0 & , & 0 \\ 0 & , & 0 & , & 0 & , & 0 \\ gB_3K_1 & , & -gB_3K_0C_1 & , & -gB_3K_0C_2 & , & -gB_3K_0C_3 \end{bmatrix} \begin{bmatrix} z \\ x_1 \\ x_2 \\ x_3 \end{bmatrix}$$

$$\begin{bmatrix} z \\ x_1 \\ x_2 \\ x_3 \end{bmatrix} + \begin{bmatrix} I_{\ell_2} \\ 0 \\ 0 \\ gB_3K_0 \end{bmatrix} v \qquad (2.40)$$

The asymptotic analysis[4] of section 2.4 can then be applied to show that

$$\begin{bmatrix} \dot{z} \\ \dot{x}_1 \\ \dot{x}_2 \\ \dot{x}_3 \end{bmatrix} = \begin{bmatrix} 0 & -C_1 & -C_2 & -C_3 \\ 0 & A_{11} & A_{12} & A_{13} \\ 0 & -R_2^{-1}R_1A_{11} & -R_2^{-1}R_1A_{12} & -R_2^{-1}R_1A_{13} \\ gB_3K_1, & -gB_3K_0C_1, & -gB_3K_0C_2, & -gB_3K_0C_3 \end{bmatrix}$$

$$\begin{bmatrix} z \\ x_1 \\ x_2 \\ x_3 \end{bmatrix} + \begin{bmatrix} 0 \\ D_1 \\ -R_2^{-1}R_1D_1 \\ 0 \end{bmatrix} d + \begin{bmatrix} I_{\ell_2} \\ 0 \\ 0 \\ gB_3K_0 \end{bmatrix} v \qquad (2.41)$$

Singular perturbation analysis[4] can now be applied to (2.41) to show that as $g \to \infty$ the closed-loop poles approach the sets

$$Z_1 = \{0 : \text{repeated } \ell_1 \text{ times}\} \qquad (2.42)$$

$$Z_2 = \{\lambda \in C: |\lambda I_{\ell_2} + K_0^{-1}K_1| = 0\} \qquad (2.43)$$

$$Z_3 = \{\lambda \in C: |\lambda I_{n-\ell_1-\ell_2} - (A_{11} - A_{13}C_3^{-1}C_1) + (A_{12} - A_{13}C_3^{-1}C_2)R_2^{-1}R_1| = 0\} \qquad (2.44)$$

$$Z_4 = \{\lambda \in C: |\lambda I_{\ell_2} + gC_3B_3K_0| = 0\} \qquad (2.45)$$

and are independent of K.

These results can be used to select R_1, R_2, K_0, K_1 and g so that all the closed-loop poles lie in the left half-plane. Further, if in such cases

$$K_0 = (C_3B_3)^{-1}\,\Sigma \qquad (2.46)$$

where $\Sigma = \text{diag}\,\{\sigma_1, \sigma_2, \ldots, \sigma_{\ell_2}\}$ and $\sigma_i \in R^+$ $(i = 1, \ldots, \ell_2)$, then analysis[34] shows that excellent tracking behaviour can be expected since the closed-loop transfer function matrix will approach the asymptotic form

$$\Gamma(\lambda) = \text{diag}\left\{ \frac{\sigma_1 g}{\lambda + \sigma_1 g}, \ldots, \frac{\sigma_{\ell_2} g}{\lambda + \sigma_{\ell_2} g} \right\} \qquad (2.47)$$

This analysis can be applied to the case of sampled-data control[5] by applying the methods of section 2.3. The results can also be extended to cases where rank $C_3B_3 < \ell_2$ by the use of inner-loop compensators.[6]

An asymptotic analysis has been presented which can be used to facilitate the selection of the appropriate feedback and controller matrices for dynamical systems in which it is feasible to use acceleration feedback. Provided that a stable closed-loop system can be obtained the results indicate that increasingly effective command input tracking and disturbance rejection characteristics can be achieved.

3. Control Application

3.1 Description of the System

At an airspeed of 50 m/s, the linearised,

small perturbation equations of motion of the longitudinal dynamics of the GARTEUR wind tunnel model[1] (flutter speed 43 m/s)includes the first three symmetric elastic modes in addition to the basic pitch and heave modes of motion and are as follows:

$$[h\ ,\ \theta] = [w\ ,\ q] \tag{3.1}$$

$$\dot{w} = -22.207\,h - 80.1775\,\theta - 37.725\,e_1 + 90.5775\,e_2 + 8.74625\,e_3 - 2.0338\,w - 0.502595\,q - 0.20045\,\dot{e}_1 - 0.009835\,\dot{e}_2 - 0.142645\,\dot{e}_3 - 15.8407\,u_t - 5.9685\,u_o - 5.105\,u_i + 1.5638\,w_g \tag{3.2}$$

$$\dot{q} = -5.681\,h - 59.354\,\theta - 23.7283\,e_1 + 64.91e_2 + 34.855e_3 - 1.22609\,w - 0.782411\,q - 0.139265\,\dot{e}_1 + 0.115725\,\dot{e}_2 - 0.450655\,\dot{e}_3 - 28.075\,u_t - 6.80575\,u_o + 0.89355\,u_i + 1.10585\,w_g \tag{3.3}$$

$$\ddot{e}_1 = -293.325\,\theta - 1147.3\,e_1 + 605.55\,e_2 + 202.223\,e_3 - 5.8665\,w - 0.8695\,q - 4.4839\,\dot{e}_1 - 0.9778\,\dot{e}_2 - 0.40889\dot{e}_3 + 39.11\,u_t - 82.11\,u_o - 32.89\,u_i + 5.8665\,w_g \tag{3.4}$$

$$\ddot{e}_2 = -145.98\,\theta - 118.445\,e_1 - 1471.35\,e_2 + 87.85\,e_3 - 2.9196\,W - 0.00375265\,q - 0.9939\,\dot{e}_1 - 2.163\,\dot{e}_2 - 0.223775\,\dot{e}_3 + 11.014\,u_t - 20.236\,u_o - 5.55075\,u_i + 2.9196\,w_g \tag{3.5}$$

$$\ddot{e}_3 = -58.4075\,\theta + 25.3925\,e_1 + 59.9775\,e_2 - 4063.23\,e_3 - 1.1659w - 0.7288\,q - 0.482065\,\dot{e}_1 - 0.455155\,\dot{e}_2 - 2.89875\,\dot{e}_3 - 43.7225\,u_t - 21.1323\,u_o + 12.8925\,u_i + 1.1659\,w_g \tag{3.6}$$

$$NZLT = \dot{w} + 0.330\,\dot{q} + 0.814\,\ddot{e}_1 + 0.739\,\ddot{e}_2 + 0.701\,\ddot{e}_3 \tag{3.7}$$

$$NZTT = \dot{w} + 0.400\,\dot{q} + 0967\,\ddot{e}_1 + 0.364\,\ddot{e}_2 + 0.620\,\ddot{e}_3 \tag{3.8}$$

$$NZLM = \dot{w} + 0.182\,\dot{q} + 0.409\,\ddot{e}_1 + 0.445\,\ddot{e}_2 + 0.230\,\ddot{e}_3 \tag{3.9}$$

$$NZTM = \dot{w} + 0.411\,\dot{q} + 0.579\,\ddot{e}_1 + 0.073\,\ddot{e}_2 + 0.101\,\ddot{e}_3 \tag{3.10}$$

$$NZG = \dot{w} - 0.059\,\ddot{e}_1 - 0.310\,\ddot{e}_3 \tag{3.11}$$

$$BMPD = -697.0\,e_1 - 877.2\,e_2 - 1390.0\,e_3 \tag{3.12}$$

$$BMMD = -247.8\,e_1 - 263.0\,e_2 - 823.1\,e_3 \tag{3.13}$$

$$BMTD = -59.58\,e_1 - 64.36\,e_2 - 282.5\,e_3 \tag{3.14}$$

In equations (3.1) - (3.14) the symbols have the meanings defined as follows:

BMPD, BMMD, BMTD - bending moments at wing pivot, wing mid-span and wing tip respectively,

e_1, e_2, e_3 - generalised displacements in the first three longitudinal symmetric elastic modes,

h - vertical displacement of the aircraft CG, positive downwards

NZLT,NZTT,NZLM,NZTM,NZG - Normal accelerations at wing tip leading edge, wing tip trailing edge, wing mid-span leading edge, wing mid-span trailing edge and fuselage centre of gravity respectively,

q - pitch rate of model, (rad/s)

u_t, u_o, u_i - taileron, outer wing flaperon and inner wing flaperon displacements, (rad.)

w - perturbation vertical velocity of model

w_g - vertical gust velocity

θ - pitch angle, (rad).

All the three actuators are described by the transfer function

$$G_A(s) = \frac{1}{1 + 2\left[\frac{0.743}{707}\right]s + \left[\frac{s}{707}\right]^2} \tag{3.15}$$

The maximum deflection of all control surfaces is to be limited to 0.1 rad. Only high pass filter dynamics are associated with the accelerometers and are described by the transfer function

$$G_F(s) = \frac{s}{s + 2} \tag{3.16}$$

The actual accelerometer dynamics are not modelled since they have a very high bandwidth.

The pitch rate gyro and its low pass filter are described by the transfer function

$$G_G(s) = \frac{1}{1 + 2\left[\frac{1.2}{100}\right]s + \left[\frac{s}{100}\right]^2} \qquad \frac{25}{s + 25} \tag{3.17}$$

The gust model used in the transient simulation studies is the 1-cosine discrete type which has the form

$$w_g(t) = \tfrac{1}{2} V \left[\frac{2\pi}{180}\right] \left[1 - \cos\left[\frac{2\pi\, t}{0.2}\right]\right] \quad 0 \leqslant t \leqslant 0.2$$

$$\text{and } w_g(t) = 0 \quad t > 0.2 \tag{3.18}$$

where V is the airspeed in m/s (ie V = 50), and Wg corresponds to a gust induced incidence change of 2 degrees.

3.2 Control Configuration

It is clear, that the system needs to be stabilised before any fine tuning can be carried out. To obtain stability, it has been 'traditional' to feed back the unstable mode(s) (in this case e_2) along with other suitable states[12]. But it is well known that flutter instability is associated with the frequency coalescence of two or more modes (either structural and/or rigid body modes) and in this

case it is the merging of the e_1 mode and e_2 mode frequencies which is associated with the e_2 mode instability. Hence, it is possible to resort to frequency separation as a means of obtaining stability for this system.

In order to carry out frequency separation, either the frequency of the e_2 mode has to be increased and/or the frequency of the e_1 mode has to be decreased. Since acceleration signals are readily measured (and have phase lead compared to either velocity or displacement signals) it is appropriate to feedback $\ddot{e}_1$ in order to increase the apparent mass of the e_1 mode and thereby reduce its frequency. This approach is shown, in this paper, to be very efficient in stabilising the system and hence there is no need to feedback e_2 in order to increase the frequency of the e_2 mode. This means that only one of the two wing flaperons is required for flutter control purposes. Since stability is achieved primarily by suppressing the frequency of the e_1 mode which consists mainly of the first bending mode of the wing, the outer wing flaperon is used as it is more effective in controlling the wing bending. As the inner wing flaperon is situated in the airframe such that it has little effect on the overall rigid body motion, it has been decided to delete completely this control surface from the integrated control structure. Hence the control input and output choices for the regulation scheme are the outer wing flaperon u_0 and $\ddot{e}_1$ respectively, that is

$$u_1 = u_0 \text{ and } a = \ddot{e}_1 \qquad (3.19)$$

It is almost certain that the model will exhibit pitching motion when encountering any disturbance and also it may become necessary to manoeuvre the model in the pitch plane. This requirement results in selecting the taileron u_t and the pitch rate q as the control input and output parameters (respectively) for the tracking scheme, that is,

$$u_2 = u_t \text{ and } y = q \qquad (3.20)$$

It is now possible to represent equations (3.1) - (3.6) in the form of equations (2.31), (2.32) and (2.33) where B_2, B_3, R_2, C_2 and C_3 are scalars.

It is evident from equations (2.42) - (2.45) that K can have any nonzero value. However, in order to increase the apparent mass corresponding to the e_1 mode (and thereby reduce the frequency of the e_1 mode), it is clear that K must also be positive. In case $K = 73.07 \times 10^{-6}$ it follows from (2.34) and (3.19) that the digital control law is given by

$$u_1 (kT) = 1/T \, (73.07 \times 10^{-6}) \; \ddot{e}_1 (kT) \qquad (3.21)$$

where T is the sampling period of equation (2.16).

Also, in case $\sigma_1 = 0.006$ and $K_1 = K_0$, it follows from (2.35), (2.36), (2.37), (2.46) and (3.20) that the digital control law is given by

$$u_2 (kT) = 1/T \, [-213.71 \times 10^{-6} \, e(kT) - 213.71 \times 10^{-6} \, z(kT)] \qquad (3.22)$$

3.3 Measurement Simplification

Of the two states that have to be obtained, the pitch rate q is by far the easier to measure using the pitch rate gyro. However, it is clear from equations (3.7) - (3.11) that $\ddot{e}_1$ can be deduced as a linear combination of the outputs of all of the five accelerometers. To ease implementational problems, it is possible to reconfigure the measurement strategy such that the number of accelerometers required can be reduced albeit with reduced accuracy of the $\ddot{e}_1$ estimate.

One way to achieve this objective is to inspect the measurement equations (3.7) - (3.11) and determine which of the sensors are to be deleted and which of the rate of change of states are to be admitted into the output thereby contaminating $\ddot{e}_1$. For each accelerometer that is deleted, at least one of the rate of states must be allowed into the output.

The following rules were adopted to reduce the number of permutations in the procedure discussed above.

1. Since, $\ddot{e}_1$ was the parameter that was required, the accelerometers which were least sensitive to picking up $\ddot{e}_1$ were deleted first from the control structure.

2. Since, feeding back $\ddot{e}_2$ would result in the reduction of frequency of the e_2 mode (with its dire consequences), $\ddot{e}_2$ was to be the last to be admitted into the output.

3. Modes with the largest frequency difference to the e_1 mode frequency (preferably the lowest frequency modes) were to be introduced first into the output to minimise modal interaction.

In the event, it was found that the number of sensors required could be reduced to just one, this vital sensor being the wing mid-span trailing edge accelerometer (NZTM). The minimal contribution from $\ddot{e}_2$ combined with a fairly high contribution from $\ddot{e}_1$ (eqn (3.10)) makes this sensor not only very useful but also rather unique.

To normalise $\ddot{e}_1$ in the output,

$$a = 1.727 \text{ NZTM} \qquad (3.23)$$

Hence in case $K = 73.07 \times 10^{-6}$ it follows from eqn. (2.34), (3.19) and (3.23) that the digital control law for the regulation scheme is given by

$$u_1 (kT) = 1/T \, (1.727 \times 73.07 \times 10^{-6}) \text{ NZTM } (kT) \qquad (3.24)$$

For the tracking scheme, of course, equation (3.22) remains unchanged.

3.4 Results and Discussion

The plan view of the GARTEUR wind tunnel model showing the locations of the control surfaces and the sensors is shown in Figure 1. The open-loop poles for the complete system are

shown in Table 1.1 and the corresponding discretized version (at T = 1/100) of the open loop poles are shown in Table 1.2.

Results have been presented for both cases of outputs in the regulation scheme discussed previously. For the first case where a = $\ddot{e}_1$(eqn. (3.19)), tables 2.1 and 2.2 show the system zeroes and the discretized closed loop poles (at T = 1/100) and figure 2 shows the associated closed loop transient responses when the model is subjected to a discrete gust (eqn. (3.18).

Similarly, for the second case where a = 1.727 NZTM (eqn. (3.23)), tables 3.1 and 3.2 show the system zeros and the discretized closed loop poles (at T = 1/100) and figure 3 shows the associated closed loop transient responses when the model is subjected to a discrete gust (eqn. (3.18)).

Examination of the two sets of results reveals that they are similar which means that little can be achieved by including in the feedback, all the other four accelerometers to the one situated in the wing mid-span trailing edge.

The changes in the system zeros are very small and the minimum phase characteristics are retained even when only NZTM is used.

The transient responses associated with the first case (a = $\ddot{e}_1$) were carried out using the digital control laws in equations (3.21) and (3.22) at an iteration rate of 100 Hz.

The transient response associated with the second case (a = 1.727 NZTM) were carried out using the digital control law in equation (3.24) for the regulation scheme, all the other control settings remaining the same.

Comparison of the two sets of transient responses reveals that the traces of h, θ, NZG and the taileron deflections are very similar in shape and magnitude. However, all the other parameters are (surprisingly) lowered in amplitude for the case when only NZTM is used.

4. Conclusions

In an attempt to combine the advantages of both theoretical and experimental approaches, the following solutions to three fundamental problems in aeroservoelasticity have been illustred:

1. A theoretical concept has been developed, which incorporates the use of the rate of change of state output feedback (with certain limitations) for regulation schemes along with the use of 'traditional' output feedback for tracking schemes, in an integrated control system.

2. The highly effective method of forcing frequency separation of frequency coalescing modes for curing flutter instability has been demonstrated.

3. A procedure for reducing the number of sensors to obtain approximations of parameters which can be difficult to measure physically has been presented.

The implementation of the control system has been greatly simplified with the deletion of the unwanted control surface u_i and sensors (in the second case). Comparison of results from previous work[2] also illustrates that acceleration feedback is highly effective in terms of maintaining low magnitudes of control surface deflections.

There are some other interesting features which can be readily related to work carried out by others:

1. The close proximity (physically) of NZTM to the outer wing flaperon seems to conform closely with the layout of control systems derived using the ILAF approach[7,8].

2. The low sensitivity of NZTM to the e_2 mode (which consists mainly of wing torsion) would indicate that NZTM is situated near the wing torsional node line. This feature has been used by other flutter suppression system designers in the past to formulate the control system architecture on the airframe[9].

3. The fuselage CG accelerometer has been widely used in both wind tunnel and flight test models[10,11] to eliminate rigid body dynamics whereas this technique was found to be unnecessary[12,13] for the discrete gust (equation (3.18)) considered in this study.

4. It is clear that in aircraft with FSW configurations, since the bending mode frequency decreases with airspeed, it is inadvisable to feedback the acceleration component of the appropriate elastic modal coordinate. A more suitable approach should invovle either elastic displacement feedback or rate of pitch rate feedback to pitching control surfaces (to reduce the frequency of the SPO mode)[9,11].

It has also been observed that the control system discussed in this paper exhibits good load alleviation characteristics.

References

1. Private Communication, "The GARTEUR Wind Tunnel Model", RAE Farnborough, February 1983.

2. Bradshaw, A., Woodhead, M. A. and Rahulan, T., "Active Flutter Suppression", MoD Research Agreement 2101/043 (XR/ST) Report, University of Salford, December 1984.

3. Leipholz, H. H. E., "Structural Control", Proc. Int. Union of Theoretical and Applied Mechanics, Ontario, June 1979.

4. Bradshaw, A. and Calderbank, J. A., "Design of Direct Digital Control Systems for Extra-long Freight Trains", 1st IASTED Int. Sym. on Applied Control and Identification, Copenhagen, June 1983.

5. Bradshaw, A. and Porter, B., "Singular Perturbation Methods in the Design of Tracking Systems Incorporating Fast-Sampling Error-Actuated Controllers", Int. J. System Sci., Vol. 12, pp. 1181-1191, 1981.

6. Bradshaw, A. and Porter, B., "Singular Perturbation Methods in the Design of Tracking Systems Incorporating Inner-loop Compensators and Fast-Sampling Error Actuated Controllers", Int. J. Systems Sci., Vol. 12. pp. 1207-1220, 1981.

7. Wykes, J. H. and Kordes, E. E., "Analytical Design and Flight Tests of a Modal Suppression System on the XB-70 Airplane", AGARD-CP-46, pp.23.1-23.18, April 1969.

8. Wykes, J. H. "B-1 Ride Control System Design Development and Test", Von Karman Lecture Series, 1979-1, 1978.

9. Rimer, M. Chipman, R. and Mercadante, R., "Divergence/Flutter Suppression System for a Forward Swept-Wing Configuration with Wing-Mounted Stores", J. Aircraft, Vol. 21, No.8, pp. 631-638, August 1984.

10. Edwards, J. W., "Flight Test Results of an Active Flutter Suppression System", J. Aircraft, Vol. 20, No.3, pp. 267-274, March 1983.

11. Noll, T. E., Eastop, F. E. and Calico, R. A., "Prevention of Forward Swept Wing Aeroelastic Instabilities with Active Controls", 14th ICAS Proceedings, pp. 439-448, 1984.

12. Thompson, G. O. and Sevart, F. D. "Wind Tunnel Investigation of Control Configured Vehicle Systems", AGARD-CP-175, pp. 4.1-4.8, July 1975.

13. Peloubet, R. P. Jr., Haller, R. L. and Bolding, R. M., "Recent Developments in the F-16 Flutter Suppression with Active Control Program", J. Aircraft, Vol. 21, No. 9, pp. 716-721, September 1984.

-525.300	±i	473.349	u_t actuator
-525.300	±i	473.349	u_o actuator
-1.421	±i	63.748	e_3 mode
+1.630	±i	37.355	e_2 mode
-5.055	±i	35.139	e_1 mode
-1.314	±i	8.148	SPO
-0.021	±i	3.531	LPO
0.000			Integrator
-2.000			HP filter
-25.000			LP filter
-53.668			pitch rate gyro
-186.332			pitch rate gyro

TABLE 1.1 OPEN LOOP POLES

Magnitude	Arg (deg)	mode
0.0052	± 88.79	u_t actuator
0.0052	± 88.79	u_o actuator
0.9859	± 36.52	e_3 mode
1.0164	± 21.40	e_2 mode
0.9507	± 20.13	e_1 mode
0.9870	± 4.67	SPO
0.9998	± 2.02	LPO
1.0000	0	Integrator
0.9802	0	HP filter
0.7788	0	LP filter
0.5847	0	Pitch rate gyro
0.1552	0	Pitch rate gyro

TABLE 1.2 OPEN LOOP POLES (DISCRETIZED AT T = 1/100)

-1.035	±i	64.366
-0.940	±i	40.260
-0.604	±i	4.301
0.000		
0.000		

TABLE 2.1 SYSTEM ZEROS FOR a = $\bar{e}_1$

Magnitude	Arg (deg)	mode
0.0052	± 88.79	u_t actuator
0.9862	± 36.62	e_3 mode
0.9931	± 22.36	e_2 mode
0.9807	± 15.17	e_1 mode
0.9845	± 4.80	SPO
0.9994	± 2.03	LPO
1.0000	0	Integrator
0.9802	0	HP filter
0.7903	0	LP filter
0.5783	0	Pitch rate gyro
0.1554	0	Pitch rate gyro
0.0057	0	u_o actuator
0.6072	180.0	u_o actuator

TABLE 2.2 CLOSED LOOP POLES FOR a = $\bar{e}_1$ (DISCRETIZED AT T = 1/100)

-1.032	± i	63.957
-0.921	± i	40.048
-0.566	± i	5.284
0.000		
0.000		

TABLE 3.1 SYSTEM ZEROS FOR a = 1.727 NZTM

Magnitude	Arg (deg)	mode
0.0052	± 88.79	u_t actuator
0.9860	± 36.39	e_3 mode
0.9928	± 22.35	e_2 mode
0.9821	± 15.17	e_1 mode
0.9864	± 4.49	SPO
0.9991	± 2.08	LPO
1.0000	0	Integrator
0.9801	0	HP filter
0.7896	0	LP filter
0.5788	0	Pitch rate gyro
0.1554	0	Pitch rate gyro
0.0057	0	u_o actuator
0.7604	180.0	u_o actuator

TABLE 3.2 CLOSED LOOP POLES FOR a = 1.727 NZTM
(DISCRETIZED AT T = 1/100)

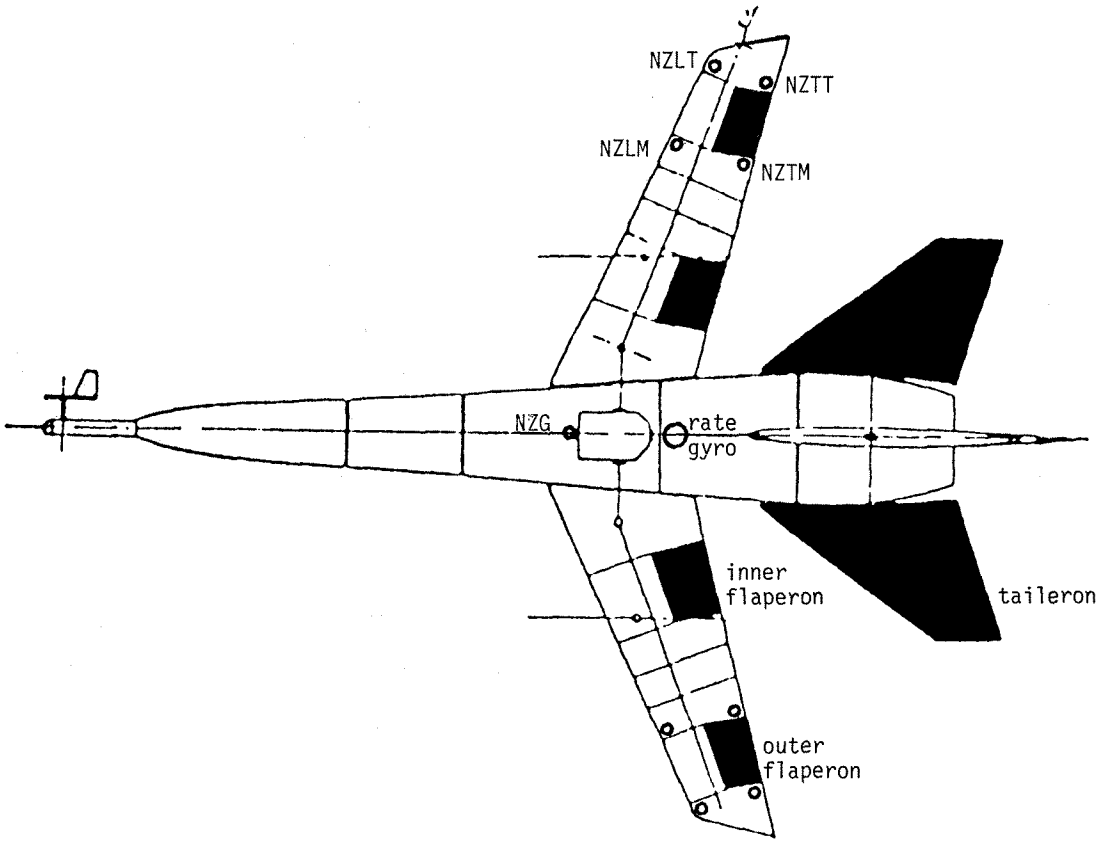

Fig.1 The GARTEUR Wind Tunnel Model showing the locations of the Accelerometers, the Pitch Rate Gyro, and the Control Surfaces.

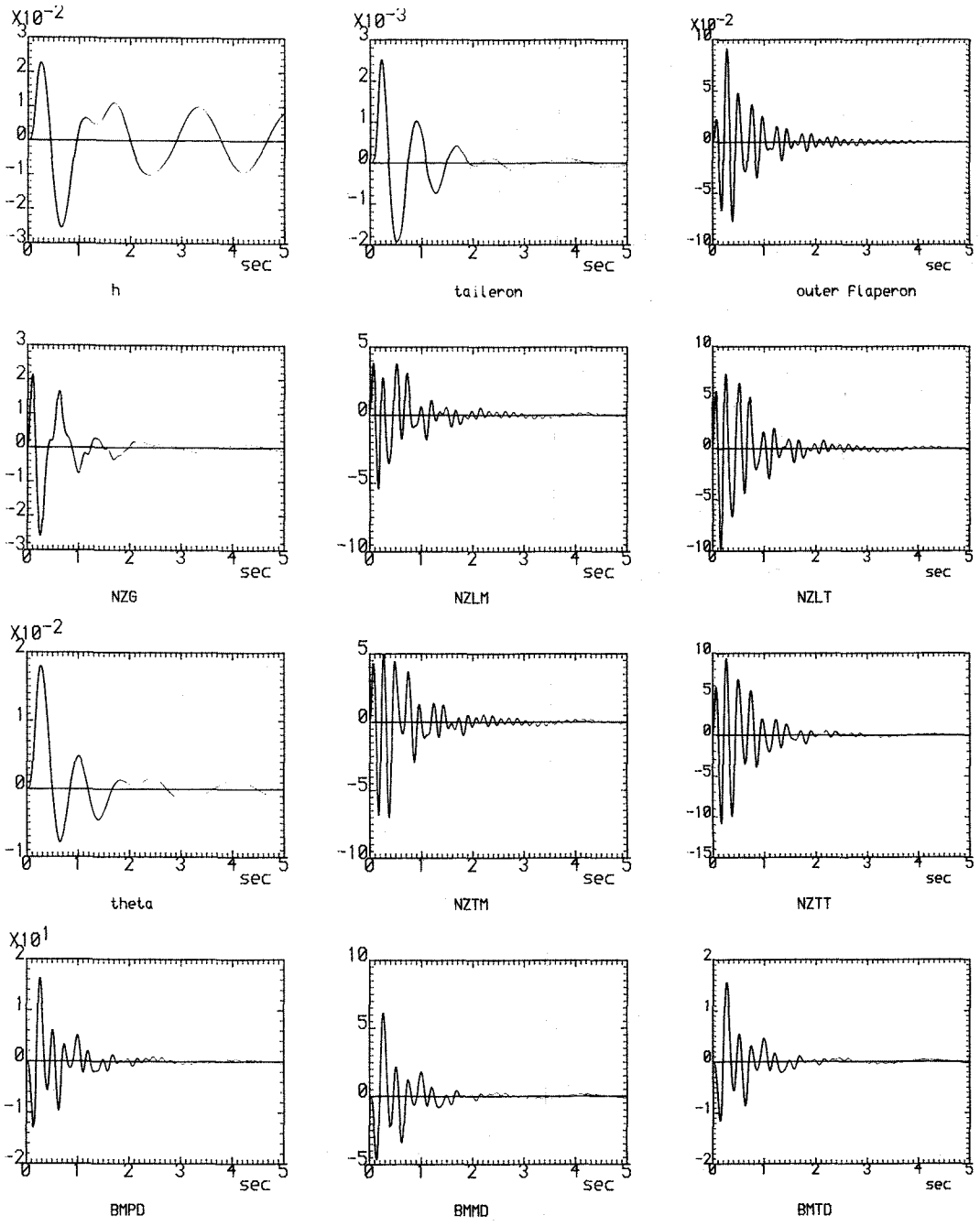

Fig.2 Transient Responses for the first case ($a=\ddot{e}_1$)

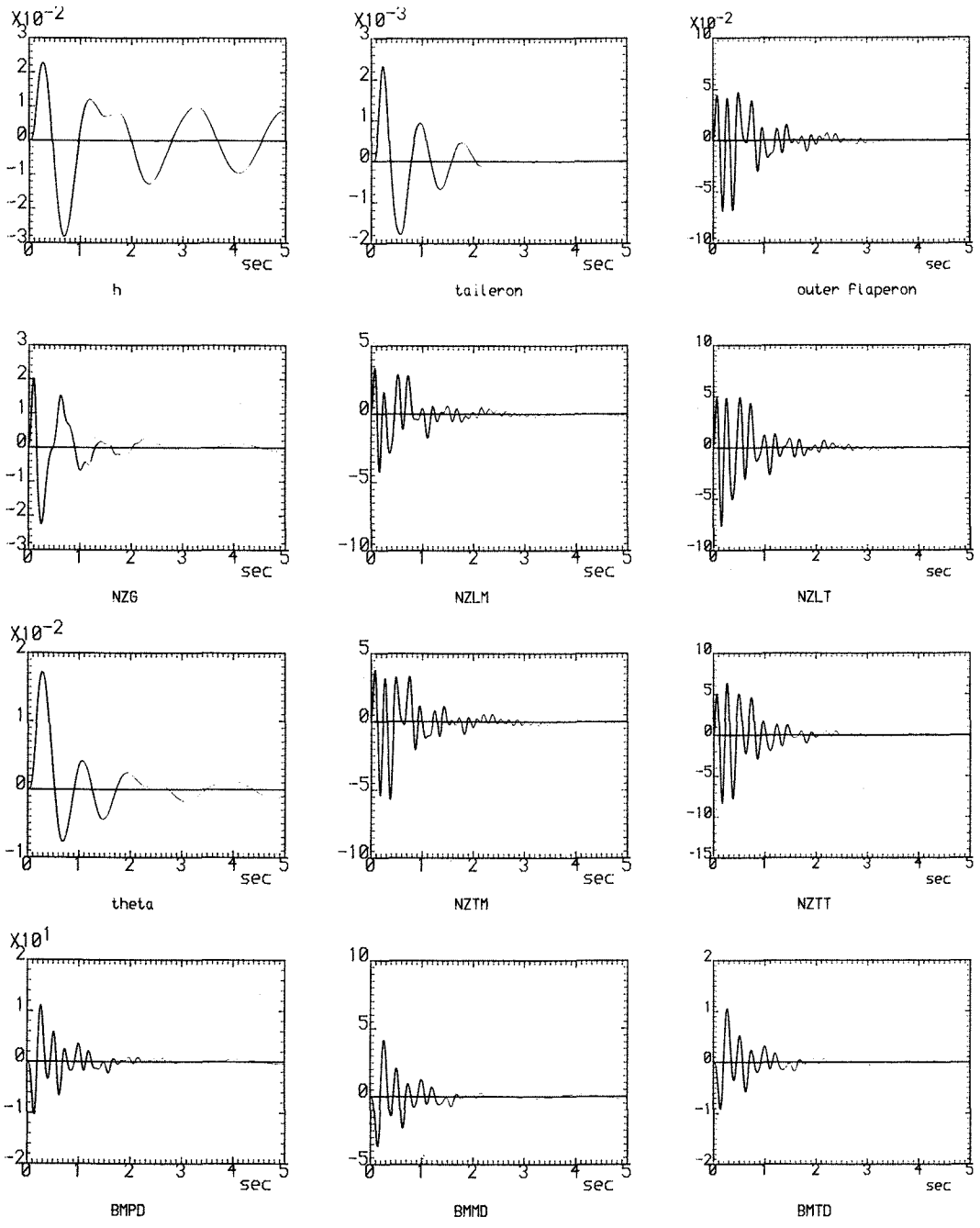

Fig.3 Transient Responses for the second case (a=1.727NZTM)